Available online at www.sciencedirect.com

ScienceDirect

Mendeleev Commun., 2020, **30**, 747–749

Mendeleev Communications

Microflow synthesis of fluorescent markers based on 1,8-naphthalimide for polylactide nanoparticles and bioimaging

Maxim S. Oshchepkov,*[a] Aleksey S. Semyonkin,[a] Alexey O. Menkov,[a] Pavel A. Melnikov,[b] Marat P. Valikhov,[b] Inna N. Solovieva,[a] Sergey V. Tkachenko[a] and Julia A. Malinowskaya[b]

[a] *D. I. Mendeleev University of Chemical Technology of Russia, 125047 Moscow, Russian Federation. E-mail: maxim.os@mail.ru*

[b] *V. P. Serbsky National Medical Research Centre of Psychiatry and Narcology, 119034 Moscow, Russian Federation*

DOI: 10.1016/j.mencom.2020.11.019

Two strategies for the synthesis of the new fluorescent markers based on 1,8-naphthalimide under classical conditions (in a flask) and in a microflow reactor are compared and contrasted. The microflow method provides higher purity of products, better productivity and production time. The resulting markers were used to obtain fluorescently labeled polylactide-based nanoparticles that can be used to study the distribution of polylactide nanoparticles as drug delivery vehicles within tissues and living organisms.

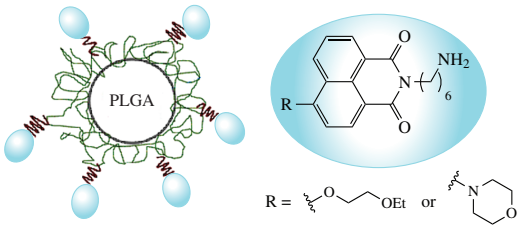

Keywords: microfluidic synthesis, fluorescent markers, polylactide, 1,8-naphthalimide, bioimaging.

Over the last several decades, the concept of targeted drug delivery and sustained release has gained much attention.[1,2] Central to this field are colloidal drug delivery systems, represented by a variety of forms (polymer micelles,[3] liposomes, microspheres, nanoparticles, *etc.*).[4–7] Polylactides are popular for the preparation of drug delivery systems.[8] Both types of polylactides: homopolymer of lactic acid and co-polymer of lactic and glycolic acids (PLGA)[9] are very promising materials for drug delivery and bioimaging.[10] Visualization plays a key role in the development of drug delivery systems, because it allows performing the direct evaluation of the distribution of a carrier in a body.[11] Covalently bound dyes are generally much less prone to leaking from drug delivery systems over significant amount of time. This has been confirmed for drug delivery systems composed of various materials (PLGA,[12,13] *N*-isopropylacrylamide,[14] silicon dioxide,[15] iron oxide,[16] *etc.*). Synthesis of new dyes possessing valuable and essential qualities such as high brightness and large Stokes shift would provide the possibility to easily discern the emitted light from the light used for excitation, reduce self-absorption, and avoid the interference of auto-fluorescence.[17,18] At the same time, incorporation of functional groups into fluorophore moiety will broaden the scope of possibilities for researchers working with drug delivery systems and biological objects.

Derivatives of 1,8-naphthalimide represent an important family of organic luminophores widely used as dyes, optical brighteners, antitumor agents, as well as fluorescent markers for synthetic polymers and textile materials.[19–23] Until now, to the best of our knowledge the synthesis of 1,8-naphthalimide derivatives in microfluidic reactors has only been reported once in our previous work.[24]

In this study, two novel fluorescent 1,8-naphthalimide derivatives with primary amino groups were synthesized and conjugated with PLGA (Scheme 1). Investigation of N-acylation and nucleophilic aromatic substitution within 1,8-naphthalic acid derivatives and optimization of the synthesis conditions in the microfluidic reactor of these compounds at each stage are the subject of the current research work.

The first step of our research included N-acylation of hexamethylenediamine with 4-substituted 1,8-naphthalic acid anhydride **1** or **4**. The use of amines for this purpose is approved by the fact that amines allow obtaining highly luminescent derivatives of naphthalimide.[19,22] Also, hexamethylenediamine has a carbon chain long enough to avoid fluorescence quenching that could occur as a result of photoinduced electron transfer and other relaxation processes.

At the first stage, we selected the optimal excess of the diamine, varying its amount in the range between 1.3 and 18 equiv., as these concentrations could allow escaping di-N-acylation (Figure 1). The concentration of compound **1** was not higher than 2.2 mM due to its low solubility in ethanol. Mixer and column temperature were set constant at 70 °C, flow ratess were 0.5 ml min^{-1}. The maximum conversion of compound **1** was reached at 8 to 10-fold molar excess of diamine, the maximum yield of product **2** was 65%, for product **5** – 68%.

When the optimal reagent excess was selected, we optimized the temperature of reaction keeping flow rates constant (see Figure S1 in Online Supplementary Materials). Based on the obtained results we have determined that the temperature change in the range of 30–80 °C has linear effect on the conversion of the initial compound **1**. At temperatures close to the boiling point of ethanol, the conversion increased by almost 10 percentage points.

Then, we selected the optimal flow rates. The reaction was conducted at reagent excess and temperature selected previously. We have found that the increase in the flow rate leads to a dramatic decrease in the conversion of the initial compound **1**. The N-acylation proceeds with incomplete conversion of initial

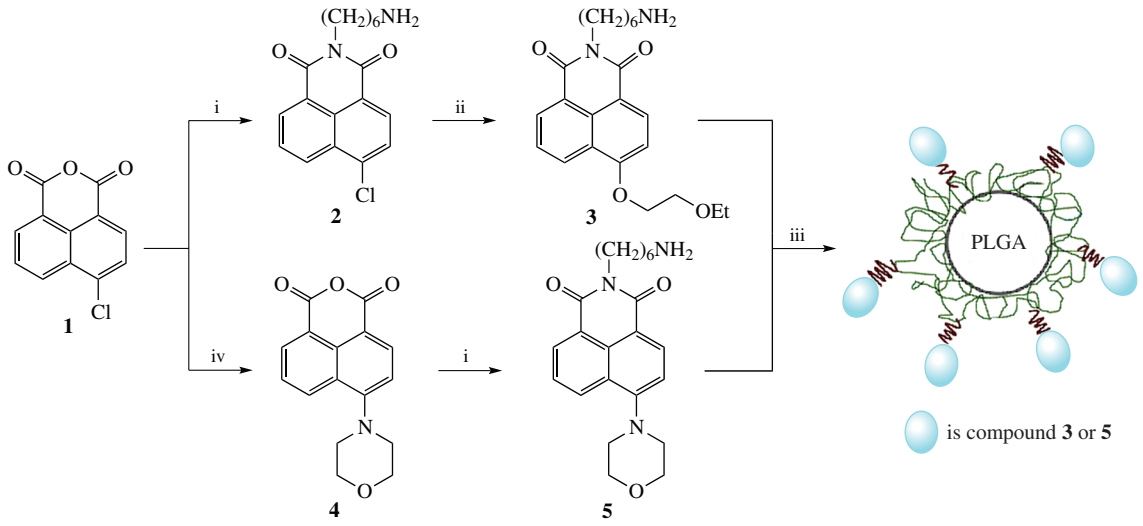

Scheme 1 *Reagents and conditions*: i, $H_2N(CH_2)_6NH_2$, EtOH; ii, $EtO(CH_2)_2ONa$, DMF or $EtO(CH_2)_2OH$; iii, PLGA, EDCI, CH_2Cl_2; iv, morpholine, DMF or $EtO(CH_2)_2OH$.

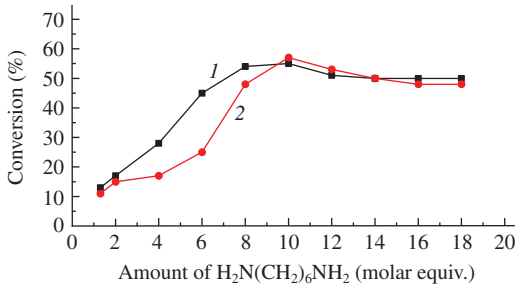

Figure 1 The dependence of conversion of the starting compounds (*1*) **1** and (*2*) **4** on the excess of hexamethylenediamine (EtOH, 70 °C).

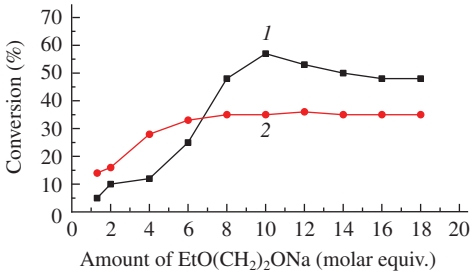

Figure 2 The dependence of conversion of the starting compound **2** on the excess of sodium 2-ethoxyethylate in the reaction held in (*1*) DMF and (*2*) 2-ethoxyethanol.

4-chloro-1,8-naphthalic anhydride **1** in a microfluidic reactor. Apparently, the reaction mixture is present in the microreactor for an insufficient period of time; thus it is not possible to achieve complete conversion. However, further reduction of the flow rate is inexpedient due to the fact that the reaction runs in a rather diluted solution. The highest yield obtained for compound **2** was 65% in a flask and 62% in a microreactor.

Similarly, the acylation was conducted to obtain compound **5**. It was performed in a T-shaped mixer with 3 ml reaction column, the temperature range was 25–78 °C. The results did not reveal a clear dependence of conversion on the reaction conditions. Apparently, kinetic studies are required to clarify this issue. Anyway, conversion of the initial compound **4** was 68% which was comparable to the yield obtained under classical conditions.

Syntheses of compounds **3** and **4** comprised nucleophilic aromatic substitution reactions of the 4-positioned chlorine atom of naphthalimide moiety. Sodium 2-ethoxyethanolate and morpholine were the reactants. Based on available data, DMF and 2-ethxyethanol were selected as solvents. The reactions were conducted at flow rates ranging from 0.1 to 2 ml min^{-1} within the temperature range of 135–155 °C. The nucleophile was used within the 3 to 15-fold molar excess range with respect to compounds **3** and **4**. In fact, the conversion of the initial compounds increased when nucleophile molar excess was raised to 5-fold, however, further raising did not improve the product yields (Figure 2).

In a microfluidic reactor, the synthesis proceeds with the conversion of the initial compound not more than 40% in 2-ethoxyethanol and 63% in DMF. When the synthesis temperature was decreased, a sharp drop in conversion was observed (see Online Supplementary Materials, Figure S2). Maximal yields of compounds **3** and **4** were observed at flow rates of 0.1 ml min^{-1} and were 63 and 65%, respectively. The yield obtained in a flask was several percent higher.

Covalent conjugation of markers **3** and **5** *via* the terminal carboxylic group of the PLGA polymer (Resomer® RG 502 H) was performed with 1-ethyl-3-(3-dimethylaminopropyl)carbodiimide and diisopropylamine (see Scheme 1 and Figure S8, Online Supplementary Materials). Absorbance and fluorescence spectra of markers **3** and **5** and the polymer with covalently bound dyes are given in Online Supplementary Materials. The obtained polymers were used to produce the nanoparticles by emulsion solvent evaporation technique. Nanoparticles with both dyes had narrow size distribution (Z-average diameter 125–135 nm, PDI ~0.150) and negative zeta potential (−20 to −30 mV). There was no significant difference as compared to the non-labeled nanoparticles produced using the same technique. Dyes **3** and **5** retain their optical properties throughout the synthesis of the conjugate and nanoparticles preparation. Moreover, fluorescence intensity does not change under both acidic and basic conditions in the pH range of 5.50–9.75, which indicates their suitability for the nanoparticles tracking *in vitro* and *in vivo*. Molar extinction coefficients and quantum yields of the dyes in solutions and in nanoparticles are presented in Table S1 (Online Supplementary Materials).

Recently, labeling of nanoparticles and intracellular targets with blue-emitting fluorescent dyes attracted more attention due to their applicability in multi-color bioimaging *in vitro* and *in vivo*.[25] Furthermore, sample labeling with fluorescent dyes with short wavelength in general provides a higher resolution in fluorescent imaging.[26] The stability of both dyes **3** and **5** under acidic and basic conditions as well as their relatively high quantum yield give the opportunity to monitor nanoparticle intracellular trafficking in complex biological environment.

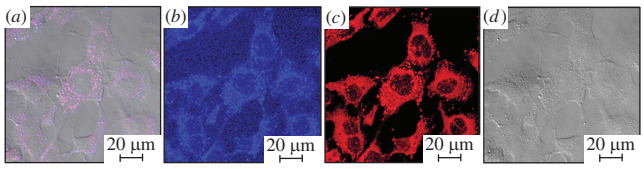

Figure 3 Confocal imaging with differential interference contrast (DIC) of 4T1 cells after incubation with the PLGA nanoparticles labeled with fluorophore **3**: (*a*) combined image, (*b*) 1 h after incubation with PLGA–**3**, (*c*) cell lysosomes stained with LysoTrackerRedDND-99 (red), (*d*) confocal visualization.

The *in vitro* distribution of the fluorescently labeled nanoparticles was investigated in live 4T1 murine mammary carcinoma cells widely used for the evaluation of anticancer therapeutics including nanoparticle-based drug delivery systems.[27,28] To track the nanoparticle intracellular distribution, the cell lysosomes were stained with LysoTracker with corresponding excitation/emission wavelength (LysoTracker Red DND-99). The LysoTracker fluorescent probes selectively label acidic organelles enabling lysosome localization in cultured cells with fluorescence microscopy.[29] Then the nanoparticles labeled with either **3** or **5** fluorescent dye were added to the cell culture medium and live cell imaging using confocal microscopy was performed within an hour. The nanoparticles labeled with either fluorophore **3** or fluorophore **5** were efficiently internalized into the 4T1 cells and partly co-localized with lysosomes. The intracellular distribution of the nanoparticles labeled with fluorophore **3** after 1 h of incubation is shown in Figure 3 (images for dye **5** are provided in Online Supplementary Materials, Figures S17–S19). It should be noted that localization in lysosomal compartment of the cells is quite common for PLGA nanoparticles.[30] The nanoparticles did not affect cell viability during the time period of the study. High fluorescence intensity and stability of the dyes embedded into the nanoparticle polymeric matrix make them suitable for fluorescence imaging using laser scanning confocal microscopy. These experiments indicate that the investigated fluorescent dyes can be used as fluorescent probes to visualize drug delivery vehicles in a wide range of biological studies.

In conclusion, microfluidic synthesis of new 1,8-naphthalimide fluorescent markers was performed. Under microflow conditions, the acylation and nucleophilic aromatic substitution do not proceed kinetically rapid enough, however microfluidic approach provides continuous regime, higher purity of products, better productivity and shorter production time. Due to high fluorescence in the blue/green region of the spectrum, stability at different pH levels, as well as to the presence of the functional amine group suitable for conjugation with the carboxylic end groups of the polymers, the obtained new 1,8-naphthalimide dyes appear to be the effective and convenient fluorescent labels for drug delivery systems.

The work was supported by the Ministry of Science and Higher Education of the Russian Federation as part of a state assignment (project FSSM-2020-0004).

Online Supplementary Materials

Supplementary data associated with this article can be found in the online version at doi: 10.1016/j.mencom.2020.11.019.

References

1 R. M. Mainardes and L. P. Silva, *Curr. Drug Targets*, 2004, **5**, 449.
2 N. Martinho, C. Damgé and C. P. Reis, *J. Biomater. Nanobiotechnol.*, 2011, **2**, 510.
3 S. R. Croy and G. S. Kwon, *Curr. Pharm. Des.*, 2006, **12**, 4669.
4 G. Barratt, *Cell. Mol. Life Sci.*, 2003, **60**, 21.
5 N. Kumskova, Y. Ermolenko, N. Osipova, A. Semyonkin, N. Kildeeva, M. Gorshkova, A. Kovalskii, T. Kovshova, V. Tarasov, J. Kreuter, O. Maksimenko and S. Gelperina, *J. Microencapsulation*, 2020, **37**, 283.
6 E. Pereverzeva, I. Treschalin, M. Treschalin, D. Arantseva, Y. Ermolenko, N. Kumskova, O. Maksimenko, V. Balabanyan, J. Kreuter and S. Gelperina, *Int. J. Pharm.*, 2019, **554**, 161.
7 R. M. Rich, D. L. Stankowska, B. P. Maliwal, T. J. Sørensen, B. W. Laursen, R. R. Krishnamoorthy, Z. Gryczynski, J. Borejdo, I. Gryczynski and R. Fudala, *Anal. Bioanal. Chem.*, 2013, **405**, 2065.
8 P. W. Lee and J. K. Pokorski, *Wiley Interdiscip. Rev.: Nanomed. Nanobiotechnol.*, 2019, doi: 10.1002/wnan.1516.
9 H. K. Makadia and S. J. Siegel, *Polymers*, 2011, **3**, 1377.
10 G. Tiwari, R. Tiwari, B. Sriwastawa, L. Bhati, S. Pandey, P. Pandey and S. K. Bannerjee, *Int. J. Pharm. Invest.*, 2012, **2**, 2.
11 J. Wang, G. Liu, K. C.-F. Leung, R. Loffroy, P.-X. Lu and X. J. Wang, *Curr. Pharm. Des.*, 2015, **21**, 5401.
12 R. Reul, N. Tsapis, H. Hillaireau, L. Sancey, S. Mura, M. Recher, J. Nicolas, J.-L. Coll and E. Fattal, *Polym. Chem.*, 2012, **3**, 694.
13 B. Weiss, U. F. Schaefer, J. Zapp, A. Lamprecht, A. Stallmach and C. M. Lehr, *J. Nanosci. Nanotechnol.*, 2006, **6**, 3048.
14 A. Auger, J. Samuel, O. Poncelet and O. Raccurt, *Nanoscale Res. Lett.*, 2011, **6**, 328.
15 B. Perlstein, T. Lublin-Tennenbaum, I. Marom and S. Margel, *J. Biomed. Mater. Res., Part B*, 2010, **92**, 353.
16 T. Tenuta, M. P. Monopoli, J. Kim, A. Salvati, K. A. Dawson, P. Sandin and I. Lynch, *PloS One*, 2011, **6**, e25556.
17 Z. Gao, Y. Hao, M. Zheng and Y. Chen, *RSC Adv.*, 2017, **7**, 7604.
18 S. Jarutikorn, S. Kraithong, J. Sirirak, W. Panchan, T. Sooksimuang and A. Charoenpanic, *Orient. J. Chem.*, 2019, **35**, 1227.
19 A. S. Oshchepkov, M. S. Oshchepkov, A. N. Arkhipova, P. A. Panchenko and O. A. Fedorova, *Synthesis*, 2017, **49**, 2231.
20 A. Oshchepkov, M. Oshchepkov, G. Pavlova, A. Ryabova, S. Kamagurov, S. Tkachenko, S. Frolova, A. Redchuk, K. Popov and E. Kataev, *Sens. Actuators, B*, 2020, 128047.
21 M. Oshchepkov, S. Tkachenko and K. Popov, *Int. J. Corros. Scale Inhib.*, 2019, **8**, 480.
22 A. S. Oshchepkov, T. A. Shumilova, M. Zerson, R. Magerle, V. N. Khrustalev and E. A. Kataev, *J. Org. Chem.*, 2019, **84**, 9034.
23 P. A. Panchenko, A. S. Polyakova, Yu. V. Fedorov and O. A. Fedorova, *Mendeleev Commun.*, 2019, **29**, 155.
24 M. Oshchepkov, I. Solovieva, A. Menkov, S. Tkachenko, V. Udovenko and K. Popov, *J. Flow Chem.*, 2020, **10**, 545.
25 N. H. Kim and D. Kim, *Blue-Emitting BODIPY Dyes*, IntechOpen, 2018, doi: 10.5772/intechopen.80349.
26 L. MacDonald, G. Baldini and B. Storrie, in *Membrane Trafficking*, 2nd edn., ed. B. L. Tang, Humana Press, New York, 2015, ch. 19, pp. 255–275.
27 A. Rivera, X. Fu, L. Tao and X. Zhang, *Int. Scholarly Res. Not.*, 2011, doi:10.5402/2011/238379.
28 P. Kaur, G. M. Nagaraja, H. Zheng, D. Gizachew, M. Galukande, S. Krishnan and A. Asea, *BMC Cancer*, 2012, **12**, 120.
29 X. Chen, Y. Bi, T. Wang, P. Li, X. Yan, S. Hou, C. E. Bammert, J. Ju, K. M. Gibson, W. J. Pavan and L. Bi, *Sci. Rep.,* 2015, **5**, 9004, doi: 10.1038/srep09004.
30 Y. Malinovskaya, P. Melnikov, V. Baklaushev, A. Gabashvili, N. Osipova, S. Mantrov, Y. Ermolenko, O. Maksimenko, M. Gorshkova, V. Balabanyan, J. Kreuter and S. Gelperina, *Int. J. Pharm.*, 2017, **524**, 77.

Received: 3rd September 2020; Com. 20/6303